

## MACRO SLIP THEORY OF PLASTICITY FOR POLYCRYSTALLINE SOLIDS\*

Wang Tsu-chiang (王自强)

(*Institute of Mechanics, Chinese Academy of Sciences, Beijing 100080, China*)

**ABSTRACT:** A macro slip theory is presented in this paper. Four independent slip systems are proposed for polycrystalline solids. Each slip system consists of a slip plane which lies on a face of the octahedron in stress space and a slip direction which is coincident with shear stress acting on the same face of the octahedron. It is proved that for proportional loading, present results are identical with the classical flow theory of plasticity. For nonproportional loading, the macro slip theory shows good predicting ability. The calculated results are in good agreement with the experimental data.

**KEY WORDS:** macro slip theory, plasticity, polycrystalline solids

### I. INTRODUCTION

The slip model is well known in the fields of the crystal plasticity. The early work given by Taylor<sup>[1]</sup>, Orowan<sup>[2]</sup>, Polanyi<sup>[3]</sup>, Schmid<sup>[4]</sup> has clearly revealed the slip mechanism of crystal.

The accurate description of deformation kinematics is due to Hill<sup>[5]</sup>, Rice<sup>[6]</sup>, Asaro<sup>[7]</sup>, Nemat-Nasser<sup>[8]</sup>, Hill and Havner<sup>[9]</sup>.

The overall elastic-plastic response of polycrystalline metals can be predicted in terms of single crystal plasticity. The classical theory is the rigid-plastic model proposed by Taylor<sup>[10]</sup> and Bishop & Hill<sup>[11]</sup>. Lin<sup>[12]</sup> developed a modified theory of Taylor model by taking account of elastic deformation.

The self-consistent model by Kröner<sup>[13]</sup> and Budiansky & Wu<sup>[14]</sup> is the first elastic-plastic theory without the assumption of uniform strain of whole polycrystalline metals and satisfying indirectly the condition of traction and displacement continuities. Hill<sup>[15]</sup> developed a new self-consistent model accounting for the plastic accommodation effect of matrix. Berveiller and Zaoui<sup>[16]</sup> modified the KBW model by taking into account the plastic accommodation effect approximately. Weng and Chiang<sup>[17]</sup> assessed influence of plastic constraint factor on polycrystal behaviour. Weng<sup>[18]</sup> proposed an anisotropic hardening formula.

On the other hand, Lin<sup>[19]</sup> presented an explicit polycrystal model to assess the overall elastic-plastic behaviour of polycrystalline metals.

The polycrystalline metal is taken as an aggregate solid in all of these theories, where complex calculations and extensive comparison with experimental data are required in order to get the material constants.

This paper presents a new macro slip theory in which the slip model will be directly applied to the description of macroscopic elastic-plastic response of polycrystalline metals. In the second section, the basic description of macro slip theory of plasticity is outlined. The proportional loading condition is analysed. It is proved that the present results are coincident with the classical flow theory for proportional loading. The general formulas for non-proportional loading of plane stress are given in the third section.

### II. BASIC DESCRIPTION

According to the Mises yield criterion, the octahedral shear stress  $\tau_8$  on any face of the

Received 17 October 1990

\* The project supported by Chinese Academy of Sciences

octahedron in the stress space is equal to  $\sigma\sqrt{2}/3$ . We can imagine that the polycrystalline solid has eight slip systems. Each slip system has a slip plane which is coincident with one face of octahedron and a slip direction which is coincident with the shear stress on the corresponding face of the octahedron. Among those eight slip systems only four slip systems are independent.

Hence the whole slip system of metallic solids consists of four independent slip systems. At any stage of deformation, these four slip systems are all determined by instantaneous stress state.

The octahedron in the stress space is shown in Fig.1. The axes of coordinate system  $OX_1X_2X_3$  are coincident with the principal axes of stresses. The unit normal  $\underline{n}^{(1)}$  of plane  $ABE$  has the components:

$$n_i^{(1)} = 1/\sqrt{3} \tag{2.1}$$

We denote a tensor with a bold letter. The matrix consisting of components of a tensor  $\mathbf{T}$  is represented by  $\underline{T}$ .

The normal stress  $\sigma_n$  on face  $ABE$  is equal to

$$\sigma_n = (\sigma_1 + \sigma_2 + \sigma_3)/3 \tag{2.2}$$

The stress vector on plane  $ABE$  is

$$\underline{f} = (\sigma_1 \ \sigma_2 \ \sigma_3)^T / \sqrt{3} \tag{2.3}$$

The shear stress vector on plane  $ABE$  is equal to

$$\underline{\tau} = \underline{f} - \sigma_n \underline{n} = (s_1 \ s_2 \ s_3)^T / \sqrt{3} \tag{2.4}$$

The octahedral shear stress  $\tau_8$  is given by

$$\tau_8 = \sqrt{s_1 * s_1 + s_2 * s_2 + s_3 * s_3} / \sqrt{3} \tag{2.5}$$

Fig.1 The octahedron in the stress space. The axes of coordinate system  $OX_1X_2X_3$  are coincident with the principal axes of stresses

the first slip system. The unit vector  $\underline{m}^{(1)}$  along slip direction of the first slip system is

$$\underline{m}^{(1)} = (s_1 \ s_2 \ s_3)^T / (\sqrt{3} \ \tau_8) \tag{2.6}$$

Similarly we have other three independent slip systems. Their slip plane normals and slip directions are given as follows:

$$\begin{aligned} \underline{m}^{(2)} &= (-s_1 \ s_2 \ s_3)^T / (\sqrt{3} \ \tau_8) \\ \underline{n}^{(2)} &= (-1 \ 1 \ 1)^T / \sqrt{3} \\ \underline{m}^{(3)} &= (-s_1 \ -s_2 \ s_3)^T / (\sqrt{3} \ \tau_8) \\ \underline{n}^{(3)} &= (-1 \ -1 \ 1)^T / \sqrt{3} \\ \underline{m}^{(4)} &= (s_1 \ -s_2 \ s_3)^T / (\sqrt{3} \ \tau_8) \\ \underline{n}^{(4)} &= (1 \ -1 \ 1)^T / \sqrt{3} \end{aligned} \tag{2.7}$$

These three slip systems lie on the plane  $BCE$ ,  $CDE$  and  $DAE$  respectively. Below the plane  $ABCD$  there are other four faces of the octahedron. The corresponding slip systems are coincident with the first four slip systems respectively. Hence there are only four independent slip systems altogether.

The plastic deformation rate  $\underline{D}^p$  can be expressed as

$$\underline{D}^p = \sum_{\alpha=1}^4 \underline{P}^{(\alpha)} \dot{\gamma}^{(\alpha)} \quad \alpha = 1, \dots, 4 \tag{2.8}$$

where

$$\underline{P}^{(\alpha)} = \frac{1}{2} (\underline{m}^{(\alpha)} \otimes \underline{n}^{(\alpha)} + \underline{n}^{(\alpha)} \otimes \underline{m}^{(\alpha)}) \tag{2.9}$$

Obviously the slip systems are determined by instantaneous stress state and vary with the stress state.

For proportional loading, the principal axes of stresses are kept unchanged. The resolved shear stress  $\tau^{(\alpha)}$  acting on the four slip systems are always equal to  $\tau_8$ . Meanwhile the increment  $\Delta\tau^{(\alpha)}$  of the resolved shear stress is also always equal to  $\Delta\tau_8$ . Therefore all slip shear rates should be identical.

We have

$$\underline{D}^p = \sum_{\alpha=1}^4 \underline{P}^{(\alpha)} \dot{\gamma}^{(\alpha)} = \dot{\gamma} \sum_{\alpha=1}^4 \underline{P}^{(\alpha)}$$

After some manipulations, we obtained

$$\underline{D}^p = \frac{4\dot{\gamma}}{3\tau_8} \begin{bmatrix} s_1 & 0 & 0 \\ 0 & s_2 & 0 \\ 0 & 0 & s_3 \end{bmatrix}$$

$$\underline{D}^p = \frac{4\dot{\gamma}}{3\tau_8} \underline{S} \tag{2.10}$$

Eq. (2.10) means that the components of plastic deformation rate tensor are proportional to deviatoric stress components. That is the essential feature of the classical flow theory of plasticity.

According to the classical flow theory of plasticity, we have

$$\underline{D}^p = \lambda \underline{S} = \frac{3\dot{\bar{\epsilon}}_p}{2\sigma_e} \underline{S} \tag{2.11}$$

Compare the Eqs. (2.10) and (2.11), it follows

$$\dot{\gamma} = \frac{3}{4\sqrt{2}} \dot{\bar{\epsilon}}_p = \frac{3\dot{\sigma}_e}{4\sqrt{2} E_t} \tag{2.12}$$

where  $E_t$  is the tangent modulus of uniaxial tension curve, and

$$E_t = d\sigma_e / d\bar{\epsilon}_p \tag{2.13}$$

### III. NONPROPORTIONAL LOADING

We start discussing a two-dimensional problem. As shown in Fig.2, a thin wall cylinder of metals is subjected to axial compression (or tension) and torsion.

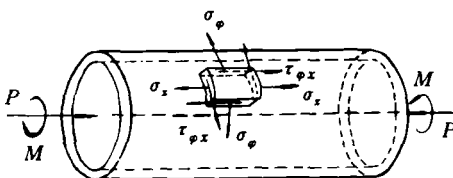


Fig.2 The thin wall cylinder of metal is subjected to axial compression (or tension) and torsion

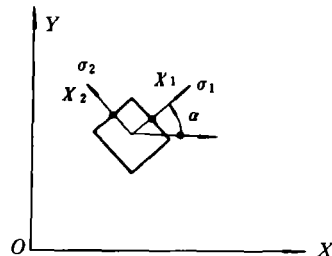


Fig.3 The angle  $\alpha$  between  $X$ -axis and the axis of the first principal stress

Principal stresses can be expressed as

$$\begin{aligned}\sigma_1 &= (\sigma_x + \sigma_y)/2 - \sqrt{(\sigma_x - \sigma_y)^2/4 + \tau_{xy}^2} \\ \sigma_2 &= (\sigma_x + \sigma_y)/2 + \sqrt{(\sigma_x - \sigma_y)^2/4 + \tau_{xy}^2}\end{aligned}\quad (3.1)$$

Let  $\alpha$  denote the angle between  $x$ -axis and the axis of the first principal stress as shown in Fig.3. We have

$$\operatorname{tg} \alpha = 2 \tau_{xy} / \{ (\sigma_x - \sigma_y) - \sqrt{(\sigma_x - \sigma_y)^2 + 4 \tau_{xy}^2} \} \quad (3.2)$$

Let  $\underline{e}_x, \underline{e}_y$  and  $\underline{e}_z$  be the base vectors of coordinate system  $OXYZ$  and  $\underline{e}_1, \underline{e}_2$  and  $\underline{e}_3$  be the base vectors of principal axes of stresses. We find that

$$\begin{aligned}\underline{e}_1 &= \cos \alpha \underline{e}_x + \sin \alpha \underline{e}_y \\ \underline{e}_2 &= -\sin \alpha \underline{e}_x + \cos \alpha \underline{e}_y \\ \underline{e}_3 &= \underline{e}_z\end{aligned}\quad (3.3)$$

The transform matrix  $\underline{Q}$  can be expressed as

$$\underline{Q} = \begin{bmatrix} \cos \alpha & -\sin \alpha & 0 \\ \sin \alpha & \cos \alpha & 0 \\ 0 & 0 & 1 \end{bmatrix} \quad (3.4)$$

Hence we obtain

$$\begin{aligned}\underline{\dot{m}}^{(\alpha)} &= \underline{Q} \underline{\dot{m}}^{(\alpha)} \\ \underline{\dot{n}}^{(\alpha)} &= \underline{Q} \underline{\dot{n}}^{(\alpha)}\end{aligned}\quad (3.5)$$

In detail, we have

$$\begin{aligned}\underline{\dot{m}}^{(1)} &= (s_1 \cos \alpha - s_2 \sin \alpha, s_1 \sin \alpha + s_2 \cos \alpha, s_3)^T / (\sqrt{3} \tau_8) \\ \underline{\dot{m}}^{(2)} &= (-s_1 \cos \alpha - s_2 \sin \alpha, -s_1 \sin \alpha + s_2 \cos \alpha, s_3)^T / (\sqrt{3} \tau_8) \\ \underline{\dot{m}}^{(3)} &= (-s_1 \cos \alpha + s_2 \sin \alpha, -s_1 \cos \alpha - s_2 \sin \alpha, s_3) / (\sqrt{3} \tau_8) \\ \underline{\dot{m}}^{(4)} &= (s_1 \cos \alpha + s_2 \sin \alpha, s_1 \sin \alpha - s_2 \cos \alpha, s_3) / (\sqrt{3} \tau_8)\end{aligned}\quad (3.6)$$

$$\begin{aligned}\underline{\dot{n}}^{(1)} &= (\cos \alpha - \sin \alpha, \sin \alpha + \cos \alpha, 1) / \sqrt{3} \\ \underline{\dot{n}}^{(2)} &= (-\cos \alpha - \sin \alpha, -\sin \alpha + \cos \alpha, 1) / \sqrt{3} \\ \underline{\dot{n}}^{(3)} &= (-\cos \alpha + \sin \alpha, -\sin \alpha - \cos \alpha, 1) / \sqrt{3} \\ \underline{\dot{n}}^{(4)} &= (\cos \alpha + \sin \alpha, \sin \alpha + \cos \alpha, 1) / \sqrt{3}\end{aligned}\quad (3.7)$$

where  $\underline{\dot{m}}^{(\alpha)}$  is the column matrix of the vector  $\dot{m}^{(\alpha)}$  in the coordinate system  $OXYZ$  and  $\underline{\dot{m}}^{(\alpha)}$  is column matrix of the vector  $\dot{m}^{(\alpha)}$  in the coordinate system  $OX_1X_2X_3$ , etc.

The Schmid hardening law can be expressed as

$$\begin{aligned}\dot{\tau}^{(\alpha)} &= \sum_{\beta=1}^4 h_{\alpha\beta} \dot{\gamma}^{(\beta)} & \dot{\gamma}^{(\alpha)} > 0 \\ & & \alpha = 1, \dots, 4 \\ \dot{\tau}^{(\alpha)} &\leq \sum_{\beta=1}^4 h_{\alpha\beta} \dot{\gamma}^{(\beta)} & \dot{\gamma}^{(\alpha)} = 0\end{aligned}\quad (3.8)$$

where  $h_{\alpha\beta}$  are the hardening coefficients which depend on the strain history.

Here we emphasize that the resolved shear stress rate  $\dot{\tau}^{(\alpha)}$  is referred to the updated slip

plane. It means that we calculate the resolved shear stress rate on the slip plane which is fixed on time  $t$ . On the next time  $t + \Delta t$ , the new slip systems may lie on the faces of new octahedron. But we take the resolved shear stress  $\tau^{(\alpha)} + \Delta \tau^{(\alpha)}$  on the original slip plane at time  $t$ . For the nonproportional loading the  $\dot{\tau}^{(\alpha)}$  will not equal to each other. But in the case of plane stress, we can prove that

$$\begin{aligned} \dot{\tau}^{(1)} &= \dot{\tau}^{(3)} \\ \dot{\tau}^{(2)} &= \dot{\tau}^{(4)} \end{aligned}$$

For the sake of simplicity, we discuss only the case in which all slip systems are continuously acting. The stress rate tensor  $\dot{\underline{\sigma}}$  has components in the coordinate system of the principal axes of stresses:

$$\dot{\underline{\sigma}} = \begin{bmatrix} \dot{\sigma}_1 & \dot{\tau}_{12} & 0 \\ \dot{\tau}_{12} & \dot{\sigma}_2 & 0 \\ 0 & 0 & 0 \end{bmatrix}$$

where  $\dot{\sigma}_1, \dot{\sigma}_2, \dot{\tau}_{12}$  are the components of stress rate tensor  $\dot{\underline{\sigma}}$  on the coordinate systems of the principal axes of stresses. On the other hand, the orientation tensors of slip systems take the forms

$$\underline{\mathbf{P}}^{(1)} = \frac{1}{3\tau_8} \begin{bmatrix} s_1 & (s_1 + s_2)/2 & (s_1 + s_3)/2 \\ (s_1 + s_2)/2 & s_2 & (s_2 + s_3)/2 \\ (s_1 + s_3)/2 & (s_2 + s_3)/2 & s_3 \end{bmatrix} \tag{3.9}$$

$$\underline{\mathbf{P}}^{(3)} = \frac{1}{3\tau_8} \begin{bmatrix} s_1 & (s_1 + s_2)/2 & -(s_1 + s_3)/2 \\ (s_1 + s_2)/2 & s_2 & -(s_2 + s_3)/2 \\ -(s_1 + s_3)/2 & -(s_2 + s_3)/2 & s_3 \end{bmatrix} \tag{3.10}$$

Noting

$$\begin{aligned} \dot{\tau}^{(1)} &= \dot{\underline{\sigma}} : \underline{\mathbf{P}}^{(1)} = s_1 \dot{\sigma}_1 + (s_1 + s_2) \dot{\tau}_{12} + s_2 \dot{\sigma}_2 \\ \dot{\tau}^{(3)} &= \dot{\underline{\sigma}} : \underline{\mathbf{P}}^{(3)} = s_1 \dot{\sigma}_1 + (s_1 + s_2) \dot{\tau}_{12} + s_2 \dot{\sigma}_2 \end{aligned} \tag{3.11}$$

Hence we have  $\dot{\tau}^{(1)} = \dot{\tau}^{(3)}$ . Similarly we can prove that  $\dot{\tau}^{(2)} = \dot{\tau}^{(4)}$ .

Now we look at the Schmid hardening law. We have

$$\begin{aligned} \dot{\tau}^{(1)} &= h_{11} \dot{\gamma}^{(1)} + h_{12} \dot{\gamma}^{(2)} + h_{13} \dot{\gamma}^{(3)} + h_{14} \dot{\gamma}^{(4)} \\ \dot{\tau}^{(2)} &= h_{21} \dot{\gamma}^{(1)} + h_{22} \dot{\gamma}^{(2)} + h_{23} \dot{\gamma}^{(3)} + h_{24} \dot{\gamma}^{(4)} \\ \dot{\tau}^{(3)} &= h_{31} \dot{\gamma}^{(1)} + h_{32} \dot{\gamma}^{(2)} + h_{33} \dot{\gamma}^{(3)} + h_{34} \dot{\gamma}^{(4)} \\ \dot{\tau}^{(4)} &= h_{41} \dot{\gamma}^{(1)} + h_{42} \dot{\gamma}^{(2)} + h_{43} \dot{\gamma}^{(3)} + h_{44} \dot{\gamma}^{(4)} \end{aligned} \tag{3.12}$$

The coefficient  $h_{13}$  represents the effect of slip shear rate  $\dot{\gamma}^{(3)}$  of the third slip system on the resolved shear stress rate  $\dot{\tau}^{(1)}$  of the first slip system. We can image that it should be equal to coefficients  $h_{24}, h_{31}$  and  $h_{42}$  due to symmetry. Similarly we have

$$\begin{aligned} h_{13} &= h_{24} = h_{31} = h_{42} & h_{11} &= h_{22} = h_{33} = h_{44} \\ h_{12} &= h_{23} = h_{34} = h_{41} & h_{21} &= h_{32} = h_{43} = h_{14} \end{aligned}$$

From Eq. (3.11), it follows that

$$\begin{aligned} \dot{\tau}^{(1)} - \dot{\tau}^{(3)} &= (h_{11} - h_{31}) (\dot{\gamma}^{(1)} - \dot{\gamma}^{(3)}) + (h_{12} - h_{32}) (\dot{\gamma}^{(2)} + \dot{\gamma}^{(4)}) = 0 \\ \dot{\tau}^{(2)} - \dot{\tau}^{(4)} &= (h_{21} - h_{41}) (\dot{\gamma}^{(1)} - \dot{\gamma}^{(3)}) + (h_{22} - h_{42}) (\dot{\gamma}^{(2)} - \dot{\gamma}^{(4)}) = 0 \end{aligned}$$

The determinant of above linear homogeneous algebraic equations is

$$\Delta = (h_{11} - h_{31})^2 + (h_{12} - h_{32})^2 > 0$$

It follows that

$$\dot{\gamma}^{(1)} = \dot{\gamma}^{(3)} \quad \dot{\gamma}^{(2)} = \dot{\gamma}^{(4)}$$

Therefore the behaviour of the first two slip systems seems to be the same as the rest slip systems .

The Schmid hardening law can be represented as

$$\begin{aligned} \dot{\tau}^{(1)} &= (h_{11} + h_{13}) \dot{\gamma}^{(1)} + (h_{12} + h_{14}) \dot{\gamma}^{(2)} \\ \dot{\tau}^{(2)} &= (h_{14} + h_{12}) \dot{\gamma}^{(1)} + (h_{11} + h_{13}) \dot{\gamma}^{(2)} \end{aligned} \tag{3.13}$$

Let

$$h_0 = h_{11} \quad q_1 = (h_{12} + h_{14}) / (2h_0) \quad q_2 = h_{13} / h_0 \tag{3.14}$$

Eq. (3.13) becomes

$$\begin{aligned} \dot{\tau}^{(1)} &= h_0 \{ (1 + q_2) \dot{\gamma}^{(1)} + 2q_1 \dot{\gamma}^{(2)} \} \\ \dot{\tau}^{(2)} &= h_0 \{ 2q_1 \dot{\gamma}^{(1)} + (1 + q_2) \dot{\gamma}^{(2)} \} \end{aligned} \tag{3.15}$$

The solution of Eq.(3.15) is

$$\begin{aligned} \dot{\gamma}^{(1)} &= \{ (1 + q_2) \dot{\tau}^{(1)} - 2q_1 \dot{\tau}^{(2)} \} / (\Delta_0 h_0) \\ \dot{\gamma}^{(2)} &= \{ 2q_1 \dot{\tau}^{(1)} - (1 + q_2) \dot{\tau}^{(2)} \} / (\Delta_0 h_0) \end{aligned} \tag{3.16}$$

where

$$\Delta_0 = (1 + q_2)^2 - 4q_1^2 \tag{3.17}$$

The solution should satisfy the constraint condition :

$$\dot{\gamma}^{(1)} , \dot{\gamma}^{(2)} \geq 0$$

For proportional loading , we have  $\dot{\tau}^{(1)} = \dot{\tau}^{(2)}$  ,  $\dot{\gamma}^{(1)} = \dot{\gamma}^{(2)}$  . It results

$$\frac{d\tau}{d\gamma} = h_0 (1 + 2q_1 + q_2) = H_0$$

where  $H_0 = h_0 (1 + 2q_1 + q_2)$  .

On the other hand, from Eqs. (2.5) and (2.12) we obtain

$$\frac{d\tau}{d\gamma} = \frac{8}{9} \frac{d\sigma_e}{d\bar{\epsilon}_p} = \frac{8}{9} E_t = H_0$$

Hence the parameter  $H_0$  can be determined from uniaxial tension curve of materials .

In order to determine parameters  $q_1$  and  $q_2$  , it is necessary to get a set of experiment data . A fine set of experiment data given by Budiansky et al.<sup>[20]</sup> has been used in this paper .

At first we should specify the equivalent plastic strain  $\bar{\epsilon}_p$  . We have

$$\sigma_{ij} D_{ij}^p = \underline{\sigma} : \sum_{\alpha=1}^4 P^{(\alpha)} \dot{\gamma}^{(\alpha)} = \sum_{\alpha=1}^4 \tau^{(\alpha)} \dot{\gamma}^{(\alpha)} = \sigma_e \frac{\sqrt{2}}{3} \sum_{\alpha=1}^4 \dot{\gamma}^{(\alpha)} = \sigma_e \dot{\bar{\epsilon}}_p$$

According to the principle of work conjunction proposed by Hill<sup>[22]</sup>, we can define the equivalent plastic strain  $\bar{\epsilon}_p$  as

$$\bar{\epsilon}_p = \frac{\sqrt{2}}{3} \sum_{\alpha=1}^4 \gamma^{(\alpha)} = \frac{\sqrt{2}}{3} \Gamma \quad \Gamma = \sum_{\alpha=1}^4 \gamma^{(\alpha)}$$

Fig.4 shows the loading path for the combined compression and shear tests of 14-T4 aluminium alloy given by Budiansky et al.<sup>[20]</sup>. All loading paths are bilinear. All specimens are firstly subjected to uniaxial compression until  $\sigma_x = -1.4 \sigma_{xL}$ . Then loading takes the path along which the ratio of  $d\sigma_x/d\tau_{xy}$  keeps constant. We select the data listed in Table 1 as the standard data from which one can find the parameters  $q_1$  and  $q_2$ .

Table 1  $\frac{d\sigma_x}{d\tau_{xy}} = 1.18$

$\sigma_x$ ksi	$\tau_{xy}$ ksi	$\epsilon_x$ $10^{-3}$	$\epsilon_y$ $10^{-3}$	$\gamma_{xy}$ $10^{-3}$
0.0	0.0	0.0	0.0	0.0
5.98	0.0	0.593	0.209	0.007
10.82	0.0	1.042	0.373	0.012
15.20	0.01	1.451	0.522	0.022
19.65	0.0	1.870	0.676	0.025
24.15	0.0	2.298	0.837	0.028
27.95	0.01	2.745	1.008	0.037
30.35	0.0	3.204	1.214	0.028
31.65	0.0	3.630	1.438	0.043
32.40	0.0	4.078	1.662	0.050
33.07	0.0	4.527	1.893	0.092
33.80	0.0	5.062	2.168	0.117
33.86	0.01	5.096	2.183	0.120
34.04	0.13	5.172	2.219	0.139
34.15	0.28	5.248	2.267	0.181
34.22	0.54	5.511	2.398	0.272
34.67	0.78	5.894	2.584	0.384
35.08	1.04	6.320	2.803	0.520
35.27	1.21	6.539	2.904	0.580
35.61	1.43	6.867	3.063	0.683
36.02	1.79	7.533	3.349	0.865
36.70	2.26	8.233	3.692	1.117
36.73	2.68	8.682	3.907	1.330
37.54	3.23	9.808	4.446	1.761
38.24	3.71	10.902	4.985	2.172

Note:  $\epsilon_x$  = axial contraction  
 $\epsilon_y$  = transverse expansion  
 $\sigma_x$  = axial compressive stress

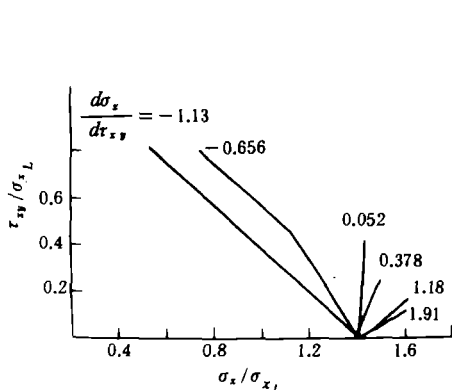


Fig.4 The loading path for the combined compression and shear tests of 14-T4 aluminum alloy given by Budiansky et al. [20]

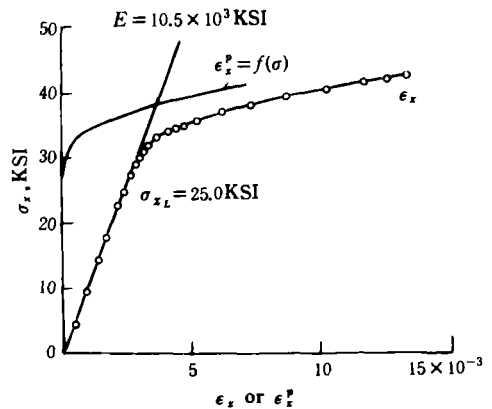


Fig.5 Stress-Strain curve in pure compression for 14-T4 aluminum alloy, after [20]

The Eq. (3.15) can be written in the incremental form :

$$\begin{aligned} \Delta \gamma^{(1)} &= \{ (1 + q_2) \Delta \tau^{(1)} - 2 q_1 \Delta \tau^{(2)} \} / (\Delta_0 h_0) \\ \Delta \gamma^{(2)} &= \{ 2 q_1 \Delta \tau^{(1)} - (1 + q_2) \Delta \tau^{(2)} \} / (\Delta_0 h_0) \end{aligned} \tag{3.18}$$

where

$$\begin{aligned} \Delta \tau^{(1)} &= \Delta \underline{\underline{\sigma}}^* : \underline{\underline{P}}^{*(1)} \\ \Delta \tau^{(2)} &= \Delta \underline{\underline{\sigma}}^* : \underline{\underline{P}}^{*(2)} \end{aligned} \tag{3.19}$$

$$\Delta \underline{\underline{\sigma}}^* = \begin{bmatrix} \Delta \sigma_x & \Delta \tau_{xy} & 0 \\ \Delta \tau_{xy} & 0 & 0 \\ 0 & 0 & 0 \end{bmatrix} \tag{3.20}$$

where  $\Delta \underline{\underline{\sigma}}^*$  and  $\underline{\underline{P}}^{*(\alpha)}$  are the matrix representations of stress increment tensor  $\Delta \sigma$  and orientation tensor  $\underline{\underline{P}}^{(\alpha)}$  in the coordinate system  $OXYZ$ .

On the other hand, we have

$$\begin{aligned} \Delta \epsilon_x^p &= (\underline{\underline{P}}_{11}^{*(1)} + \underline{\underline{P}}_{11}^{*(3)}) \Delta \gamma^{(1)} + (\underline{\underline{P}}_{11}^{*(2)} + \underline{\underline{P}}_{11}^{*(4)}) \Delta \gamma^{(2)} \\ \Delta \epsilon_{xy}^p &= (\underline{\underline{P}}_{12}^{*(1)} + \underline{\underline{P}}_{12}^{*(3)}) \Delta \gamma^{(1)} + (\underline{\underline{P}}_{12}^{*(2)} + \underline{\underline{P}}_{12}^{*(4)}) \Delta \gamma^{(2)} \end{aligned} \tag{3.21}$$

Based on Eq. (3.20) the calculation results of incremental plastic strain can be worked out.

Let

$$d = (\Delta \epsilon_x^p - (\Delta \epsilon_x^p)_{exp})^2 + (\Delta \epsilon_{xy}^p - (\Delta \epsilon_{xy}^p)_{exp})^2$$

where  $(\Delta \epsilon_x^p)_{exp}$  and  $(\Delta \epsilon_{xy}^p)_{exp}$  are the experimental results of incremental plastic strain.

Adjust the parameters  $q_1$  and  $q_2$  so that the calculated results will fit the experimental results approximately. Our calculation shows that the result that  $q_1 = -0.95$  and  $q_2 = 1.4$  gives very good prediction on the plastic response.

Using the determined parameters  $q_1$ ,  $q_2$  and  $H_0$ , one can calculate the elasto-plastic response on any loading path. The calculated results for all loading paths shown in Fig.4, are plotted in Fig.6—Fig.11. For the sake of comparison, different calculation results predicted by several theories are also shown in these figures. The solid line with small circle represents experimental data, the dashed line with short “—” represents the results of deformation theory, the dashed line with longer “—” represents the results of flow theory, symbols “◇” are the results of the slip theory proposed by Batdorf and Budiansky<sup>[21]</sup>, small triangles “▲” are the present results of the macro slip theory. It can be seen that the present theory gives the best prediction.

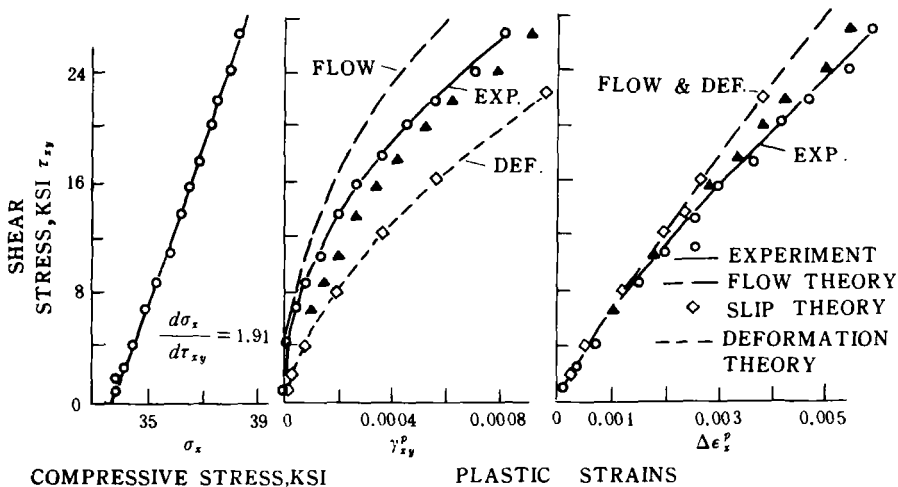


Fig.6 Loading path and plastic strain :  $d\sigma_x/d\tau_{xy}=1.91$ .  
The small triangle “▲” represents the present result



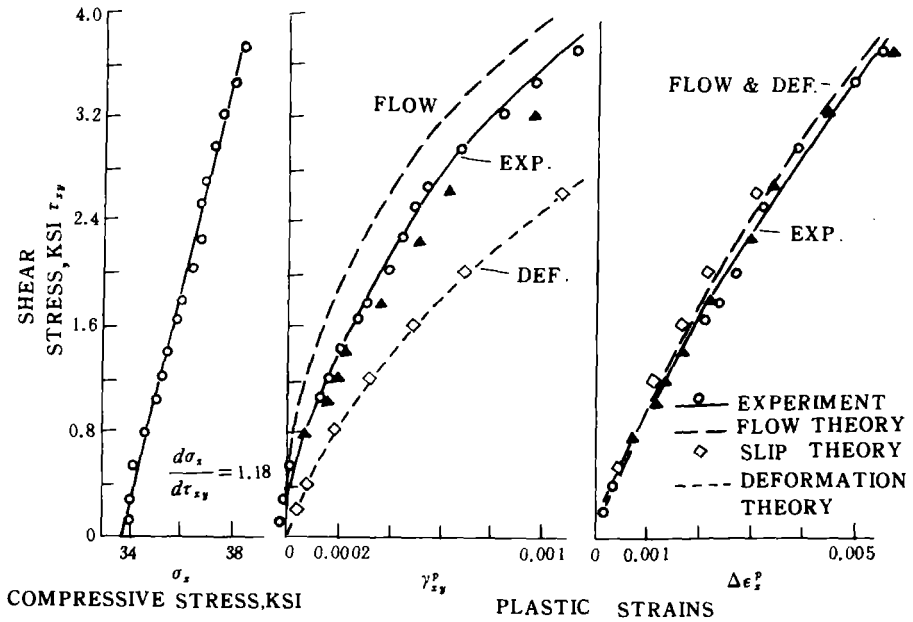


Fig.7 Loading path and plastic strain:  $d\sigma_x/d\tau_{xy}=1.18$ .  
The small triangle "▲" represents the present result

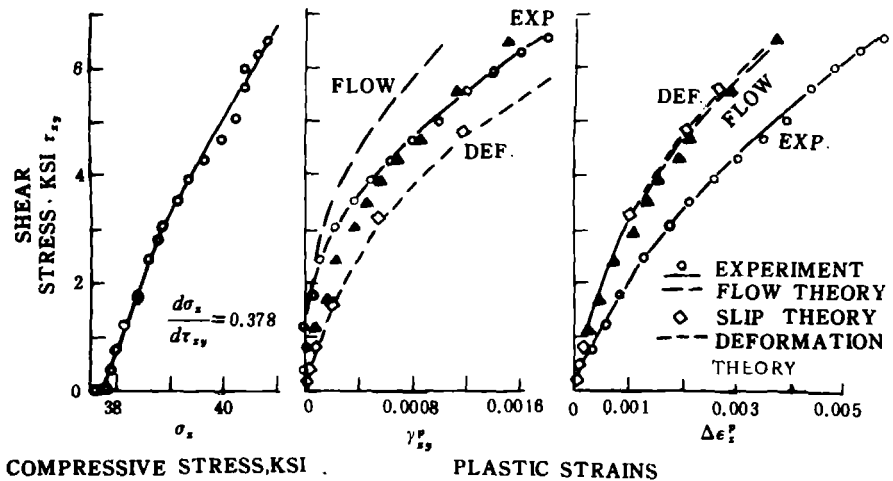


Fig.8 Loading path and plastic strain:  $d\sigma_x/d\tau_{xy}=0.378$ .  
The small triangle "▲" represents the present result

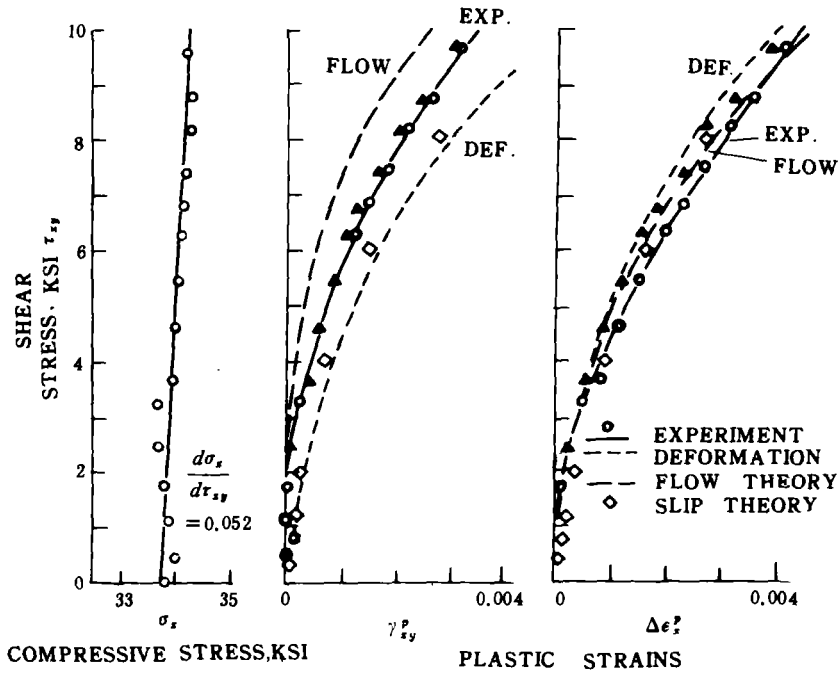


Fig. 9 Loading path and plastic strain :  $d\sigma_x/d\tau_{xy}=0.052$ .

The small triangle "▲" represents the present result

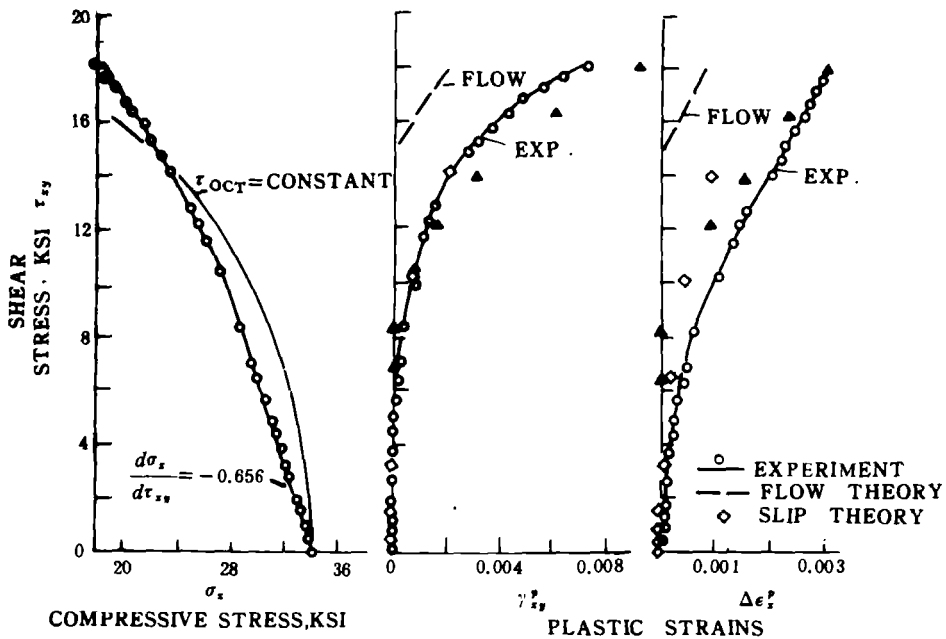


Fig. 10 Loading path and plastic strain :  $d\sigma_x/d\tau_{xy} = -0.625$ .

The small triangle "▲" represents the present result

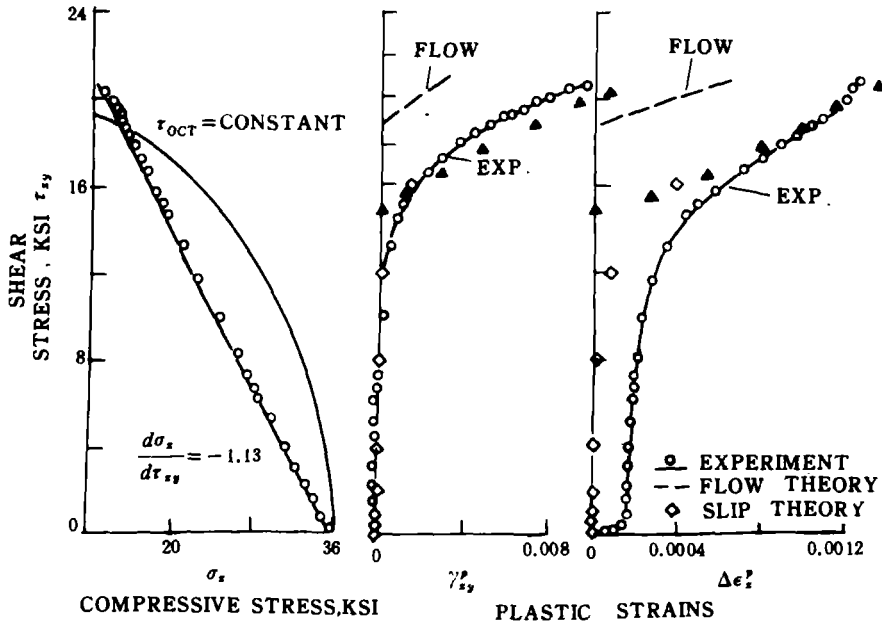


Fig.11 Loading path and plastic strain :  $d\sigma_x/d\tau_{xy} = -1.13$ .  
The small triangle "▲" represents the present result

**IV. CONCLUSION AND DISCUSSION**

The following conclusions can be drawn from this study :

1. A macro slip theory has been presented in this paper . This theory is based on the following assumption : the overall plastic response of polycrystalline metals can be described by multiple slips on four independent slip systems . Each slip system consists of a slip plane lying on a face of the octahedron in the stress space and slip direction along shear stress direction on the corresponding face .
2. For the single crystal, the slip systems are determined by the crystallographic structure and independent of the stress state . On the other hand , the macro slip theory shows significant effect of stress state on slip systems , which reflect the overall plastic response of numerous single crystal constituents .
3. The material parameters included in the macro slip theory can be determined by standard experiments . The calculation required for this theory is quite simple in comparison with the selfconsistent theory .
4. For proportional loading, the results given by the macro slip theory are coincident with the results of the classical flow theory .
5. For nonproportional loading , the macro slip theory shows good predicting ability . The predicted results are in good agreement with the experimental results given by Budiansky et al . [20] .

When a polycrystalline solid is subjected to complex loading, different single crystal constituents show different behaviour . The overall response of the plastic deformation should be determined by some kinds of averaging methods . There are two kinds of averaging methods :

- ( a ) The first one is the phenomenological approach, in which some internal variables or some complicated evolution laws of yield surface should be identified from standard experiment work .
- ( b ) The second one is the physical based approach in which the heterogeneous microstructure of polycrystalline solids must be analysed and some kind of quasi statistical description should be adopted .

The second approach is attractive from a physical point of view. But it requires complicated calculation and extensive experimental data. Meanwhile it is difficult to get the whole microstructural information of materials.

The microstructure, orientation, shape, size and properties of different single crystal constituents are completely different. The space distribution of numerous single crystal constituents is at random. Hence the problem essentially is a statistical one.

The present theory seems to belong to the phenomenological theory. But the parameters included in this theory are fairly defined and have clear physical meaning. The multiple slips on four independent slip systems are somewhat of a statistical description of multi-slips on numerous single crystal constituents.

### REFERENCES

- [1] Taylor, G.I., Proc. R. Soc. London, Series A **145** (1934), 362—387.
- [2] Orowan, E., Z. Phys., **89**(1934), 634—659.
- [3] Polanyi, Von, M., Z. Phys., **89**(1934), 660—664.
- [4] Schmid, E., Proc. Inter. Congr. Appl. Mech., 1924 (Delft), 342.
- [5] Hill, R., J. Mech. Phys. Solids, **14** (1966), 95—102.
- [6] Rice, J., J. Mech. Phys. Solids, **19**(1971), 443—455.
- [7] Asaro, R.J., Micromechanics of crystals and polycrystals, Advances in Applied Mechanics, Vol. 23, 1—115, 1983. Eds. Hutchinson, J.W. and Wu, T.Y.
- [8] Nemat-Nasser, S., J. Appl. Mech., **50** (1983), 1114—1126.
- [9] Hill, R. and Havner, K., J. Mech. Phys. Solids, **30**(1982).
- [10] Taylor, G. I., J. Inst. Metals, **62**(1938), 307—324.
- [11] Bishop, J.F.W. and Hill, R., Phil. Mag., **42**(1951), 414—427; 1298—1307.
- [12] Lin, T.H., J. Mech. Phys. Solids, **5** (1957), 143.
- [13] Kroner, E., Acta Met., **9**(1961), 155—161.
- [14] Budiansky, B. and Wu, T. T., Proc. 4th U.S. National Cong. Appl. Mech., 1962, 1175—1185.
- [15] Hill, R., J. Mech. Phys. Solids, **13**(1965), 89—101.
- [16] Berveiller, M. and Zaoui, A., J. Mech. Phys. Solids, **26**(1979), 325—344.
- [17] Weng, G.J. and Chiang, C. R., Int. J. Solids and Struct., **20**(1984), 689.
- [18] Weng, G.J., Int. J. Plasticity, **3**(1987), 315—339.
- [19] Lin, T.H., J. Engn. Mater. Tech., **106** (1984), 290.
- [20] Budiansky, B. Dow, N. F. Peters, R. W. and Shepherd, R. P., in Proceedings of 1st U. S. National Congress. Applied Mechanics, 1951, 503—512.
- [21] Batdorf, S.B. and Budiansky, B., NACA TN 1871, 1949.
- [22] Hill, R., in Advances in Appl. Mech., Vol. 18 (1978), 1.